



## Two Dimensions Enhanced Matrix Pencil for Direction of Arrival

Mohammed Amine Ihedrane<sup>1</sup>, Adiba EL Fadl<sup>2</sup>, Seddik Bri<sup>3</sup>, Nejwa El Maammar<sup>4</sup>

<sup>1,3</sup>Materials and Instrumentation, High School of Technology, Moulay Ismail University Meknes, Morocco  
amine.ihedrane@gmail.com/ seddik.bri@gmail.com

<sup>2</sup>Physics Department, Normal School Superior, Mohamed Five University, Rabat, Morocco  
adifadl@gmail.com

<sup>4</sup>Electronics Instrumentation and Measurements, Faculty of Sciences and Technologies, Errachidia, Morocco,  
nejwa.elmaammar@gmail.com

### ABSTRACT

In this article, we ameliorate the 2-D enhanced matrix pencil (2-D EMP) by employing unitary matrix transformation to reach the 2-D poles corresponding to the direction of arrival (DOA), elevation and azimuth angles using Uniform Rectangular Arrays (URA) and Uniform Circular Array (UCA). The 2-D unitary enhanced matrix pencil (2-D UEMP) allows transformation to real matrices, which can significantly, decrease the complexity of computation. Simulations results show that the accuracy of the 2-D UEMP can achieve the same results compare to 2-D EMP, then since we find azimuth and elevation angles using 2-D UEMP, The results demonstrate clearly that the Matrix Pencil investigate in this work is more accurate and stable compared to the published measure.

**Key words:** UEMP, EMP, DOA, UCA, URA, Matrix Pencil, Smart Antenna

### 1. INTRODUCTION

Nowadays, wireless telecommunications constantly researches new technologies to improve bandwidth, capacity and quality. One of the technologies that can help improve wireless systems is the smart antenna [1-2].

A smart antenna is an essential element in telecommunications systems, whose antenna pattern performance can be improved. This is done by several antennas, which are processed simultaneously. The dynamic change of the antenna pattern allows the system to beam at a target, and with this improvement in its signal to noise ratio. The beam can also be shaped to eliminate interference and multipath [3] from certain directions. Spatial separation of multiple users by multiple beams allows more users per cell because users can reuse the frequency. Here are some examples of using a smart antenna system to improve a wireless system.

The smart cities need infrastructural development and housing plan by using smart technologies for the comfortable life of the people [4]. While developing smart cities, there are many issues that need to be considered, such as population, culture, technology and growth. The main issue, however, is the high population of a city. It needs to analyze the impact of traffic and health monitoring systems. GPS has limitations such as selective availability and anti-spoofing. Instead of using GPS, an IRNSS constellation can be used to improve the quality of service wider availability across the regions. This paper is organized as follow: In Section 2, we present the previous work according to the high resolution methods in section 3, we define the properties of the centro-Hermitian matrix are presented. Then a signal model for the 2-D case is presented in section 3. 2-D UEMP is developed in section 4. Simulation results are shown in section 5, followed by the conclusion.

### 2. PREVIOUS WORK

The conventional signal processing algorithms using the covariance matrix works on the assumption that the signals impinging on the array are not coherent. Under uncorrelated conditions, the source covariance matrix satisfies the full rank condition, which is the basis of the eigen-decomposition. Many techniques involve modification of the covariance matrix through a preprocessing scheme called spatial smoothing. Recently, Hua and Sarkar [5] utilized the matrix pencil to get the DOA of the signals in a coherent multiple environments, for 2-D DOA, proposed 2-D enhanced matrix pencil (2-D EMP) method which achieves better results than the 2-D MP [6] and then the EMP [7].

In order to reduce the computational complexity of calculations, Huang and Yeh [8] have developed a unitary transform; this algorithm has a reduced computational complexity, because it is based on the real-valued computations at all stages. Many works [9] applied Unitary Transformation to ESPRIT; moreover, unitary ESPRIT achieves automatic pairing, sono pair-matching procedure is needed. Also, in [10] it's shown that TLS-ESPRIT estimate accurately 2-D DOA in the uncorrelated sources, For all raisons listed above, the main aim of this paper is to apply 2-D. UEMP to determinate azimuth and elevation angles

impinging on Uniform Rectangular and Circular Array, then smart Antenna directs the principal beam towards the desired signal by using Zero forcing method [11].

### 3. CENTRO-HERMITIAN MATRIX

A square  $N \times N$  matrix,  $B$ , is called unitary, if it satisfies  $B^{-1} = B^H$ . The superscript  $H$  denotes the complex conjugate transpose of a matrix. Where  $A$ , is the centro-hermitian, if it satisfies:

$$A = \prod_P A^* \prod_S \quad (1)$$

$\prod_P$  is called the exchange matrix and defined as

$$\prod_P = \begin{bmatrix} 0 & \dots & 0 & 0 & 1 \\ 0 & \dots & 0 & 1 & 0 \\ 0 & \dots & 1 & 0 & 0 \\ \vdots & \ddots & \vdots & \vdots & \vdots \\ 1 & \dots & 0 & 0 & 0 \end{bmatrix}_{P \times P} \quad (2)$$

Here  $\prod_P$  is  $P \times P$  square matrix, and  $A^*$  is conjugate of  $A$ .

Theorem 1: If the matrix  $A$  is centro-hermitian, then  $Q_P^H A Q_S$  is a real matrix. Here the matrix  $Q$  is unitary, whose columns are conjugated symmetric and has a sparse structure [13]. For  $P$  even, we have:

$$Q_P = \frac{1}{\sqrt{2}} \begin{bmatrix} I & iI \\ \prod & -i\prod \end{bmatrix} \quad (3)$$

Here,  $I$  and  $\prod$  are matrices that have the dimension of  $P/2$  and  $i = \sqrt{-1}$ .

When  $P$  is odd, we have:

$$Q_P = \frac{1}{\sqrt{2}} \begin{bmatrix} I & 0 & iI \\ 0 & \sqrt{2} & 0 \\ \prod & 0 & -i\prod \end{bmatrix} \quad (4)$$

*Proof 1:* Using  $\prod_P \prod_P = I$ , the conjugate of  $Q_P^H A Q_S$  is  $(Q_P^H A Q_S)^* = Q_P^T A^* Q_S^* = Q_P^T \prod_P \prod_P A^* \prod_S \prod_S Q_S^*$  Since

$$\prod_P Q^* = Q \quad \text{and} \quad \prod_P A^* \prod_S = A$$

$$(Q_P^H A Q_S)^* = Q_P^H A Q_S \quad (5)$$

Therefore,  $Q_P^H A Q_S$  is a real matrix.

### 4. SIGNAL MODEL

In order to define the signal model, we have used two networks. The first one is the *Uniform Rectangular Array* (URA) and the second one is *Uniform Circular Array* (UCA). We assume that there are  $N$  antenna with  $M$  is the

narrow band far field signals from different incident direction. The radius of the circular array is denoted as  $r$  and wavelength of narrow band is  $\lambda$ . The incident angle of the signals is shown in figure.1.

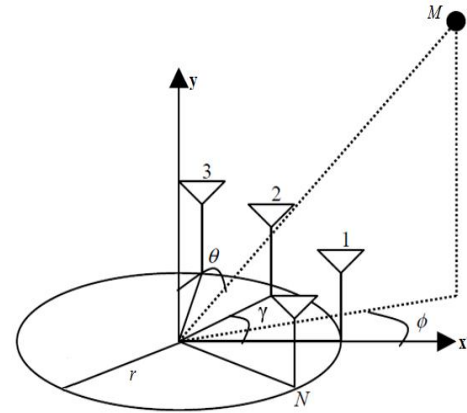


Figure.1: Uniform circular array[12]

Consider a uniform rectangular array of  $M \times N$  unidirectional sensor elements shown in figure. 2. With  $\Delta x$  and  $\Delta y$  are the sensor spacing in  $x$  and  $y$  direction, and for simplicity we assume that  $\Delta = \Delta x = \Delta y$ .

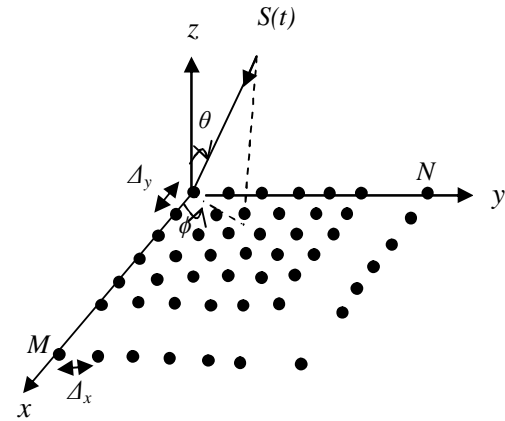


Figure. 2:  $M \times N$  uniform rectangular array

The narrow-band plane waves arrive at this uniform rectangular array, with an elevation angle ( $\theta$ ) and the azimuth angle ( $\phi$ ). Then the signal received at the sensor ( $m, n$ ) is as follows:

$$X_{(m,n)}(t) = Z_{(m,n)}(t) + n_{(m,n)}(t) \quad (6)$$

$$\begin{aligned} X_{(m,n)}(t) &= \sum_{p=1}^d a_p e^{j\gamma_p} \exp\left\{j \frac{2\pi\Delta}{\lambda_0} \left\{ (m-1)\cos\phi_p \right. \right. \\ &\quad \left. \left. + (n-1)\sin\phi_p \right\} \sin\theta_p\right\} + n_{(m,n)}(t) \\ &= \sum_{p=1}^d a_p e^{j\gamma_p} \exp\left\{j \left\{ (m-1)\psi_{xp} + (n-1)\psi_{yp} \right\}\right\} + n_{(m,n)}(t) \end{aligned} \quad (7)$$

The signal model has  $P$ , 2-D exponential signals, where  $a_p$  and  $\gamma$  are the magnitudes and the phases respectively,  $d$  is number of signals, and  $n(m,n)$  indicates additive White Gaussian Noise.

### 5. 2-D UNITARY ENHANCED MATRIX PENCIL (2-D UEMP)

The Hankel matrix  $Z^{(i,j)}$  is defined as:

$$Z^{(i,j)} = \begin{bmatrix} Z_{(i,j)} & \cdots & Z_{(1,N-m_1+j)} \\ \vdots & & \vdots \\ Z_{(M-m_2+i,j)} & \cdots & Z_{(M-m_2+i,N-m_1+j)} \end{bmatrix} \quad (8)$$

Where  $m_1$  is the first pencil parameter ( $d \leq m_1 \leq M-d$ ) and  $m_2$  is the second pencil parameter ( $d \leq m_2 \leq N-d$ ).

By using theorem 1, we can write:

$$Z_r = Q^H Z_{ch} Q \quad (9)$$

Where  $Z_r$  is real valued matrix.

$$Q^H J_2 Q Z_r = \alpha_x Q^H J_1 Q Z_r \quad (10)$$

Hence,

$$(Q^H J_1 Q)^* Z_r = \alpha_x Q^H J_1 Q Z_r \quad (11)$$

With:

$$\{ \text{Re}(Q^H J_1 Q) - j \text{Im}(Q^H J_1 Q) \} Z_r = \{ \text{Re}(\alpha_x) + j \text{Im}(\alpha_x) \} \times \{ \text{Re}(Q^H J_1 Q) + j \text{Im}(Q^H J_1 Q) \} Z_r \quad (12)$$

Since,  $\alpha_x = e^{j\psi_{xi}}$  :

$$\text{Re}(\alpha_x) = \text{Re}(e^{j\psi_{xi}}) = \cos(\psi_{xi}) \quad (13)$$

$$\text{Im}(\alpha_x) = \text{Im}(e^{j\psi_{xi}}) = \sin(\psi_{xi})$$

Therefore:

$$\tan\left(\frac{\psi_{xi}}{2}\right) \text{Re}(Q^H J_1 Q) Z_r = \text{Im}(Q^H J_1 Q) Z_r \quad (14)$$

In the real case, the signal is contaminate with noise, so  $Z_r$  matrices are constructed from the noisy data  $X_{(m,n)}$  in equation (6).

Now the singular value decomposition (SVD) of real  $Z_r$ , can be written as:

$$Z_r = U \Sigma V^H = U_s \Sigma_s V_s^H + U_n \Sigma_n V_n^H \quad (15)$$

Where  $U_s$ ,  $\Sigma_s$  and  $V_s^H$  are in the signal subspace corresponding the  $d$  principal components whereas  $U_n$ ,  $\Sigma_n$  and  $V_n^H$  are in the noise subspace.  $\Sigma$  is the singular values of  $Z_r$ , which are located on the main diagonals in the descending order  $\sigma_1 \leq \sigma_2 \leq \dots \leq \sigma_d$ .  $d$  is number of the signals. If the data is noiseless, the first  $d$  singular values are nonzero, the rest is zero, where:

$$\sigma_i > 0 \quad \text{for } i=0, 1, \dots, d,$$

$$\sigma_i = 0 \quad \text{for } i=d+1, \dots, \min(m_1 (M-m_2+1), m_2 (N-m_1+1)) \quad (16)$$

If the data is noisy,  $d$  needs to be estimated, The ratio of each of the singular value to the largest one determines the value of  $d$ . the signal subspace has dimension  $d$  that corresponds to the main eigen-values of  $\Sigma$  and the noise subspace that is related to the rest of eigen-values. In order to reduce the effect of the noise, the equation (14) can be written as:

$$\tan\left(\frac{\psi_{xi}}{2}\right) \text{Re}(Q^H J_1 Q) U_s = \text{Im}(Q^H J_1 Q) U_s \quad (17)$$

Then:

$$\psi_{xi} = 2 \tan^{-1}(\alpha_x) \quad (18)$$

As before:

$$\tan\left(\frac{\psi_{yi}}{2}\right) \text{Re}(Q^H J_3 Q) Z_r = \text{Im}(Q^H J_3 Q) Z_r \quad (19)$$

We use left singular eigenvector  $V_s$

$$\tan\left(\frac{\psi_{yi}}{2}\right) \text{Re}(Q^H J_3 Q) V_s = \text{Im}(Q^H J_3 Q) V_s \quad (20)$$

Then:

$$\psi_{yi} = 2 \tan^{-1}(\alpha_y) \quad (21)$$

Once  $\psi_{xi}$  and  $\psi_{yi}$  are estimated, the elevation and azimuth angles are obtained from the following equations, without correct pairing:

$$\begin{cases} \theta_i = \text{Arc sin} \left[ \frac{-j\lambda_0}{2 \pi \Delta} \sqrt{(\text{Ln } \psi_{xi})^2 + (\text{Ln } \psi_{yi})^2} \right] \\ \phi_i = \text{Arctg} \left[ \frac{\text{Ln } \psi_{yi}}{\text{Ln } \psi_{xi}} \right] \end{cases} \quad (22)$$

$i = 1, 2, \dots, d$

The proposed estimation method is summarized as follows:

**Step1:** From the data signal, find a particular Enhanced Matrix  $Z^{(i,j)}$ .

**Step2:** Compute the real data matrix  $Z_r$ .

**Step3:** Compute the SVD of  $Z_r$ , and calculate left and right singular vectors  $U_s$  and  $V_s$  (respectively), which the  $d$  largest singular vectors of  $Z_r$  are.

**Step4:** Calculate the generalized eigenvalues of the matrix  $\text{Im}(Q^H J_1 Q) U_s$  and  $\text{Re}(Q^H J_1 Q) U_s$  to find  $\alpha_x$  and the generalized eigenvalues of the matrix  $\text{Im}(Q^H J_3 Q) V_s$  and  $\text{Re}(Q^H J_3 Q) V_s$  to find  $\alpha_y$ .

**Step5:** Calculate azimuth and elevation angles using (22).

### 6. RESULTS AND SIMULATIONS

For all simulations, the signals have a phase of  $\gamma_i=0$  degrees, and are contaminate with a zero mean Gaussian white noise with variance  $\sigma^2$ . The distance between the antenna elements is  $\Delta=\Delta x=\Delta y=\lambda/2$ . In this paper the Cramer-Rao Bounds (CRB) is employed for performance comparison. The CRB provides a lower limit on the variance obtainable by any technique as a function of the Fisher information matrix (FIM) and the estimator's bias gradient. The theoretical CRB for the 2D-DOA cases was developed in [11].

**In the first step**, we choice of the pencil parameter, there is a value of L which, in the case where the signal has only one real component, minimize the variant of the estimator. Its optimal value is:

$$L = \frac{N}{2} \tag{23}$$

One can find an analytical expression of the variance of the estimator in the case of a single frequency:

$$x = R e^{j\omega t} \tag{24}$$

In this case, the equation 24 leads to the following result:

$$\text{Var} \delta \omega = \frac{\sigma^2}{|S|^2} \begin{cases} \frac{1}{L(N-L)^2} & \text{si } L \leq N/2 \\ \frac{1}{L^2(N-L)} & \text{si } L \geq N/2 \end{cases} \tag{25}$$

Then we demonstrate that there exist, for a given value of number of antenna N, two optimal values for the parameter L which are:

$$L = N/3 \quad \text{et} \quad L = 2N/3 \tag{26}$$

In order to prove this solution, we have used Two coherent signals are impinging on URA with  $\theta = [45^\circ, 55^\circ]$  and  $\phi = [30^\circ, 40^\circ]$ . The numbers of antenna elements are  $M=N=20$ . This simulation results are based on 800 Monte Carlo runs and one snapshot. The SNR=20 dB. Different values of m1 and m2 are plotted along the x-axis and the inverse of the sample variance of the estimates of theta (elevation angle) and phi (azimuth angle) in logarithmic domain for 2-D UEMP and 2-D EMP method is shown along the y-axis in figure 3.

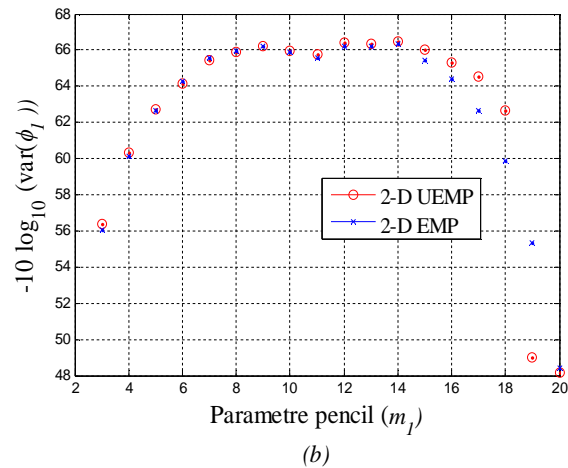
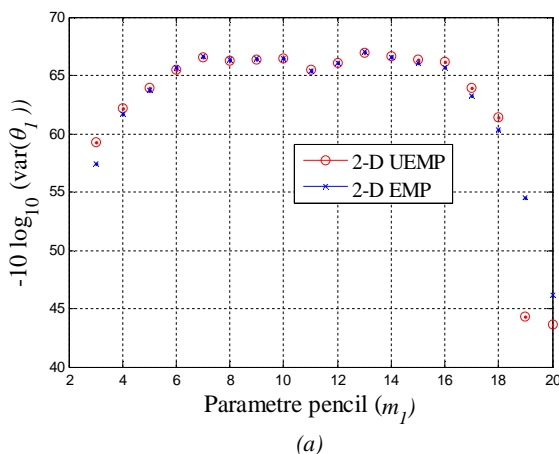


**Figure.3:** Sample variance of the estimated angles as function of pencil parameter

From figure 3, it is easy to observe that the pencil method for the two methods 2-D UEMP and 2-D EMP is the most sensitive to noise when the free parameter pencil is equal to d (number of impinging signal) and N – d or M-d. Figure 3 (a) and (b) show that 9 and 12 are the best choices for m1 figure 3 (c) show that 9 and 11 are the best choices for m2. In fact, all values satisfying  $(N/3 \leq m1 \leq 2N/3)$  appear to be good choices in general. This phenomenon can be seen in all other cases of  $\theta, \phi$  and SNR. In the following examples the parameters pencil are chosen to be  $m1=m2=9$  because they are the optimum choice for the two methods when  $M=N=20$  or  $M=N=19$ , and  $m1=m2=8$  when  $M=N=18$ .

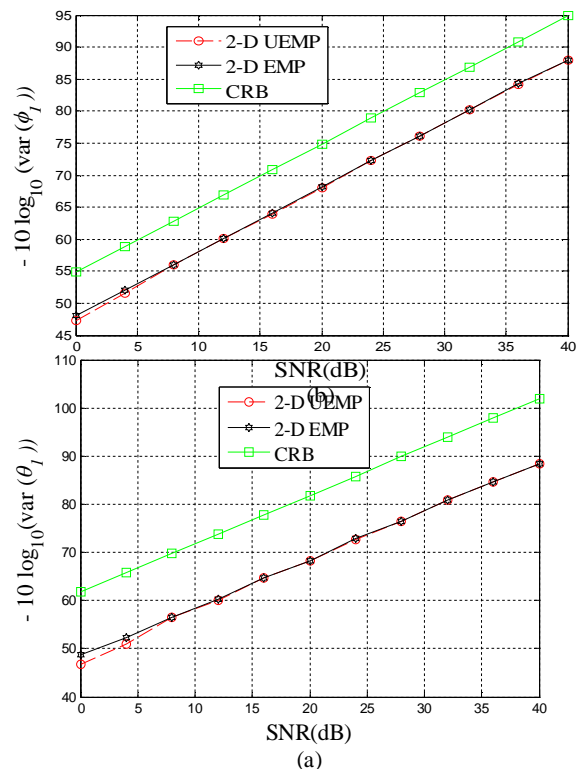


**Figure.4:** Sample variance of the estimated angles as function of SNR, 20\*20 antennas

There are two coherent signals are impinging on URA with  $\theta = [45^\circ, 55^\circ]$  and  $\phi = [30^\circ, 40^\circ]$ . The numbers of antenna elements are  $M=N=20$ . The first pencil parameter  $m_1=9$  and the second pencil parameter  $m_2=9$ . This simulation results is based on 800 Monte Carlo runs and one snapshot. Different values of SNR are plotted along the x-axis and the inverse of the sample variance of the estimates of theta (elevation angle) and phi (azimuth angle) in logarithmic domain for 2-D UEMP and 2-D EMP is shown along the y-axis in figure.4.

**In the second step**, we chose the upgrade the performances of the 2-D UEMP using URA geometry . for that we chose two coherent signals are impinging on URA with  $\theta=[45^\circ,55^\circ]$  and  $\phi=[30^\circ,40^\circ]$ .The numbers of antenna elements are  $M=N=18$ . The first pencil parameter  $m_1=8$  and the second pencil parameter  $m_2=8$ . This simulation results is based on 800 Monte Carlo runs and one snapshot. Different values of SNR are plotted along the x-axis and the inverse of the sample variance of the estimates of theta (elevation angle) and phi (azimuth angle) in logarithmic domain for 2-D UEMP and 2-D EMP is shown along the y-axis in figure. 5.

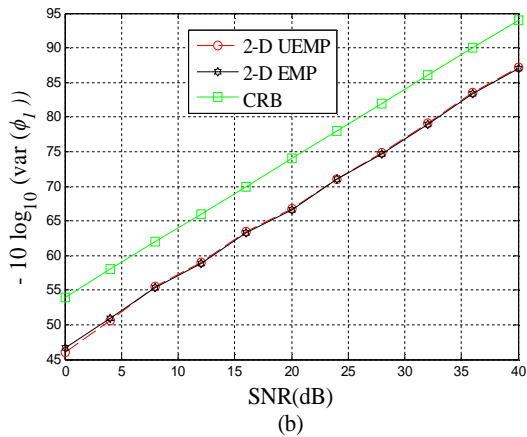
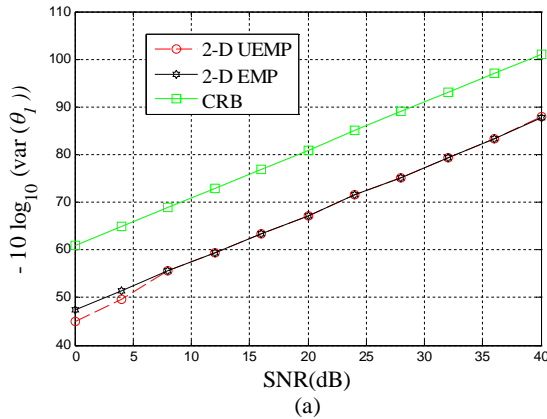


**Figure.5:** Sample variance as function of SNR an 18\*18 antennas

In the figures 4 and 5, 2-D UEMP shows comparable performance than 2-D EMP except for small SNR region.

## 7. DISCUSSION

In this section, we analyze the Matrix Pencil investigated at this research and compared with the experimented one [13-15] for circular array of eight circular sector antennas, with  $d = 0.6 \lambda$ . This network receives the desired signal at an angle of 50 degrees, interference at angles of 25 and 80 degrees and the SNR = 20 dB.

In the figure .6 we plots the spectrums of three functions including 2-D UEMP [13], and the proposed estimator. It is seen from the figures that the proposed method estimates  $\Psi$  correctly, which generates corresponding peaks at  $\Psi_1 = \sin(\theta_1) \cos(\phi_1) = \sin(10) \cos(20) \approx 0.16$ ,  $\Psi_2 = \sin(\theta_2) \cos(\phi_2) = \sin(30) \cos(35) \approx 0.41$  and  $\Psi_3 = \sin(\theta_3) \cos(\phi_3) = \sin(40) \cos(150) \approx -0.56$ .as expected. This indicates that can be estimated efficiently by the method with 2-D spectral search.

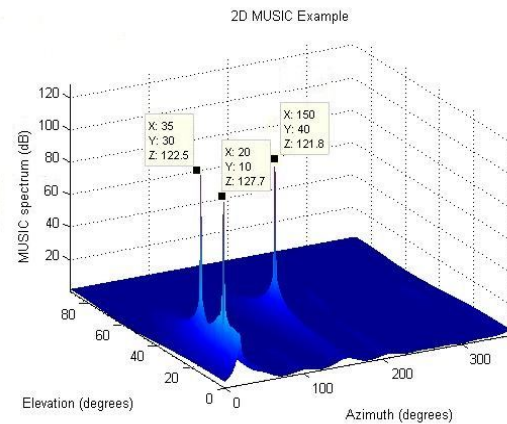


**Figure.6.** Matrix Pencil for azimuth and elevation (10, 20) (30, 35) and (40,150)

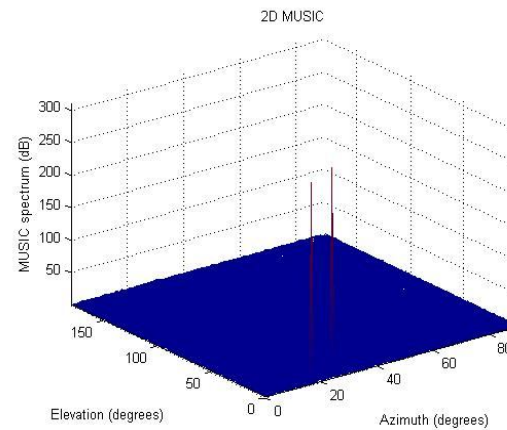


**Figure.7:** Matrix Pencil using 4 elements with central antenna

Figure.7 present that after determined angles by using 2-D Matrix Pencil method, the proposed geometry directs the main beam towards the user and at the same time forms nulls in the directions of interferers in the case of two and tree signals.

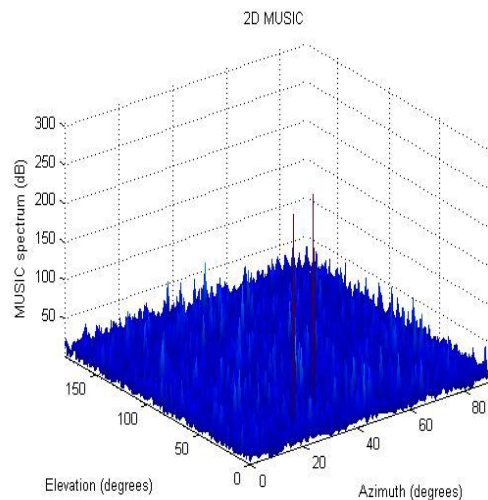
**Table 1:** Comparative results for different signals

Signal	$\theta_{in}$	$\theta_{out}$	$\Delta\theta_{out}$	$\varphi_{in}$	$\varphi_{out}$	$\Delta\varphi_{out}$	
1	[15]	78	78.5	+0.0064	128.4	129.5	+0.0082
		84	82.5	0	116.0	117	+0.0086
	2-D UEMP	78	78	0	128.4	128.1	-0.0023
		84	84	0	116.0	116.2	+0.0017
2	[15]	77.0	76.0	-0.0065	128.2	129.5	77.0
		85.8	86.5	0	120	121.5	85.8
	2-D UEMP	77.0	77.0	0	128.2	128.2	00
		85.8	85.8	0	120	120.1	+0.0008
3	[15]	78.6	0	-1	133.6	0	-1
		82.4	0	-1	137.8	0	-1
	2-D UEMP	78.6	79.0	+0.005	133.6	134	+0.0029
		82.4	85.4	+0.036	137.8	137	-0.0028

From the table 1, we observe that the proposed method estimates 3 DOA more accurately while the experimented one cannot detect angles when the Number of signals exceeds 2. The proposed one gives a less error margin to estimate DOA.

We observe also that 2-D Matrix Pencil using the proposed geometry can be applied for correlated sources to eliminate multipath (when the antenna receives the desired signal and its various multipath components).

The figure.8 confirm that the 2-D UEMP can resolve clearly the angles ( $\theta, \varphi$ ) and the peaks become Sharp. Both of the two algorithms can get a correct estimation of the direction angle of independent signals. Because of re-constructing the data covariance matrix in the modified algorithm, which is equivalent to utilize the information of the data one more time, the peak of spectrum becomes sharper and the precision is higher [14].


**Figure.8:** Pencil algorithm using 4 elements

## 8. CONCLUSION

A new 2-D UEMP is employed to estimate the arrival angles impinging on URA and UCA arrays. This algorithm converts the complex data matrix to a real matrix so the computational load is reduced. Besides, the pair-matching procedure of the angles is automatic, which also reduce the computational load. It is seen that for lower SNR of the data, 2-D EMP performs better than 2-D UEMP, after a certain threshold, both of them show comparable performance. The proposed method can estimate 2-D DOAs in the case of correlate and uncorrelated sources. The proposed method can be apply in many applications like smart antenna, computer simulations show that when the 2-D DOAs are accuracy estimate by 2-D UEMP smart antenna.

## REFERENCES

1. A.J. Van Der Veen, M.C. Vanderveen, A. Paulraj, **Joint angle and delay estimation using shift invariance techniques**, IEEE trans. signal process. Vol.46.No.2.pp. 405-418. 1998.
2. Aaron Don M.*et all* . **Sensor-based Traffic Control Network with Neural Network Based Control System**, International Journal of Advanced Trends in Computer Science and Engineering, Vol.8 No. 4,pp.983 – 989.2019
3. T.K. Sarkar, M.C. Wicks, M. Salazar-Palma, **Smart Antennas**, Wiley, 2003.
4. J. B Andersen, N. Blaustein, **Multipath phenomena in cellular network**, Artech house publishers, 2002.
5. A. Y. J. Chan, J. Litva, **MUSIC and maximum likelihood techniques on two-dimensional DOA estimation with uniform circular array**, IEE Proceedings Radar, Sonar and Navigation. Vol.142.No3. pp.105-114.1995.
6. K. C. Huang, C. C. Yeh, **Unitary transformation method for angle of arrival estimation**, IEEE Trans. Signal Process. 39 (4) (1991) 975-977.
7. T.K. Sarkar, O. Pereira, **Using the matrix pencil method to estimate the parameters of a sum of complex exponentials**, IEEE Antennas Propag. Mag. Vol.37.No1.pp48–54. 1994.
8. M.A.Ihdrane, S.Bri. **Direction of Arrival Using Uniform Circular Array based on 2-D MUSIC Algorithm**, Indonesian Journal of Electrical Engineering and Computer Science .Vol 12.N°1. pp. 30-37 .2018.
9. S.Mubeen, **Synthesis of Circular Array Antennas Using Accelerated Particle Swarm Optimization** , International Journal of Advanced Trends in Computer Science and Engineering,Vol.8 No. 4,pp.2121 – 2125.2019.
10. M. A.Ihdrane, S. Bri, **Two-Dimension MUSIC Algorithm Using Uniform Circular Array** ,International Journal of Information Science & Technology .Vol.2 No.2, pp. 29-34, 2018.
11. M.A. Ihdrane, S.Bri. **Direction of Arrival Estimation using MUSIC, ESPRIT and Maximum- Likelihood Algorithms for Antenna Arrays**, Walailak Journal of Science and Technology, Vol 13,N°6. pp. 491-502.2015

12. M.A.Ihdrane ,S.Bri,A. El Fadl,High **Resolution Method using Patch Circular Array**, International Journal of Electrical and Computer Engineering . Vol. 7, No. 4 , pp. 2116-2124 , 2017.
13. P. Zhao, G. Hu, and L. Wang. **A Dimensionality Reduction MUSIC Method for Joint DOA and Polarization Estimation in the PRDRF System Using SSSC-EVSA**. PIER M, , Vol.75, pp.39-48. 2018
14. C.R. Karanam, et all. **Magnitude-Based Angle-of-Arrival Estimation, Localization, and Target Tracking**, Inter.Conf. Info Proc. Sens. Netw.pp.254-265.2018.
15. M.A. Ihdrane, A ElFadl and Se.Bri. **Direction of Arrival Using 2-D Matrix Pencil Method**.Advances in Science, Technology and Engineering Systems Journal, Vol.4.No.5, pp.341-345.2019.